Adopted Levels, Gammas

Q(β^-)=10470 *40*; S(n)=2470 *40*; S(p)=18680 *40*; Q(α)=−13690 *40* 2021Wa16
S(2n)=10020 *40*, S(2p)=33930 *40*, Q(β^-n)=2090 *40* (2021Wa16).
Isotope discovery (2012Th10): ^{232}Th(^{40}Ar,X) at Dubna (1971Ar32).
^{35}Si production:
2015Mo17: ^{9}Be(^{40}Ar,X) at E(^{40}Ar)=95 MeV/nucleon at RIKEN. Measured angular distributions and transverse momentum distributions of fragments. Deduced formulation for the width of transverse momentum distribution as a function of fragment velocity.
2012Kw02: ^{9}Be,^{nat}Ni,^{181}Ta(^{40}Ar,X) at E(^{40}Ar)=140 MeV/nucleon at NSCL. Measured fragmentation cross sections, parallel momentum transfers, and widths. Compared with empirical formula EPAX, and predictions from internuclear cascade and deep inelastic models using Monte Carlo ISABEL-GEMINI and DIT-GEMINI codes.
2012Zh06: ^{9}Be,^{181}Ta(^{40}Ar,X) at E(^{40}Ar)=57 MeV/nucleon at HIRFL. Measured momentum distributions and production cross sections of fragments. Observed competition between projectile fragmentation and other mechanisms. Compared with EPAX, abrasion- ablation, and HIPSE models. Studied target dependence of fragment cross sections.
2007No13: ^{9}Be(^{40}Ar,X) at E(^{40}Ar)=100 MeV/nucleon at RIKEN. Measured fragment momentum distributions and production cross sections.
2006Ro34: ^{2}H(^{42}S,X) at E(^{42}S)=99.8 MeV/nucleon at NSCL. Measured production cross sections.
1997Fo01: ^{208}Pb(^{37}Cl,X) at E(^{37}Cl)=230 MeV at Legnaro. Measured yields.
^{35}Si decay measurements:
1986Du07,1986HuZW,1987DuZU,1988DuZS,1988DuZT: ^{9}Be(^{40}Ar,X) at GANIL. Measured $T_{1/2}$ and β^--delayed γ rays.
2007Ne14: ^{35}Si g.s. magnetic moment and g-factor using β-NMR.
^{35}Si radius measurements:
2006Kh08: ^{35}Si produced by ^{181}Ta(^{48}Ca,X) fragmentation at E(^{48}Ca)=60.3 MeV/nucleon at GANIL. Measured energy-integrated reaction cross sections at 30-65 MeV/nucleon using a silicon telescope as both active target and detector. Deduced reduced strong absorption radii, isospin dependence, and possible halo structure or large deformation.
1999Ai02: Si(^{35}Si,X) at NSCL. Measured energy-integrated reaction cross sections at E=38-80 MeV/ nucleon. Deduced strong absorption radii.
^{35}Si mass measurements: 1986Fi06, 1986Sm05, 1984Ma49.
Theoretical calculations (binding energies, deformation, quadrupole moments, radii, levels, J^π, etc.): 2011Ka03, 2009No01, 2008Wi11, 2007Ch82, 2004Kh16, 1999Du05, 1994Mo37, 1994Po05, 1987Wa10, 1986Wo02.

^{35}Si Levels

Cross Reference (XREF) Flags

A ^{35}Al β^- decay (38.1 ms)
B ^{36}Al β^-n decay (12.0 ms)
C ^{37}Al β^-2n decay (11.4 ms)
D ^{2}H(^{34}Si,pγ)
E ^{9}Be(^{36}Si,^{35}Siγ)

E(level)†	J$^\pi$‡	$T_{1/2}$	XREF	Comments
0	(7/2)$^-$	0.78 s *12*	ABCDE	%β^-=100; %β^-n<5 (1995ReZZ/2008ReZZ) μ=(−)1.638 *4* (2007Ne14,2014StZZ) μ: Using β-NMR on a polarized fragment beam (2007Ne14). J$^\pi$: (d,p)=3 in ^{2}H(^{34}Si,pγ), 7/2$^-$ from shell-model predictions, and systematic trends in Si isotopes. $T_{1/2}$: From β-decay measurement (1988DuZT). In an earlier paper by the same group (1986Du07) value given is 0.87 s *17*. The evaluators adopt the more recent value. Reduced strong absorption radius r_0^2=1.261 fm^2 *35* from the energy-integrated σ of Si(^{35}Si,X) (2006Kh08) and r_0^2=1.258 fm^2 *92* from the energy-integrated σ of Si(^{35}Si,X) (1999Ai02). Configuration=$\nu f_{7/2}$.
909.95 *23*	(3/2)$^-$	55 ps *14*	ABCDE	$T_{1/2}$: from (^{36}Si,^{35}Siγ). J$^\pi$: L(d,p)=1 in ^{2}H(^{34}Si,pγ), 3/2$^-$ from shell-model predictions, and systematic

Continued on next page (footnotes at end of table)

Adopted Levels, Gammas (continued)

^{35}Si Levels (continued)

E(level)[†]	J$^\pi$[‡]	T$_{1/2}$	XREF	Comments
				trends in Si isotopes.
				T$_{1/2}$: From analysis of broadened lineshape in ^{9}Be(^{36}Si,^{35}Siγ) (2014St18). Configuration=νp$_{3/2}$.
973.88 *18*	(3/2$^+$)	5.9 ns *6*	A E	T$_{1/2}$: from ^{35}Al β^- decay (38.1 ms). T$_{1/2}$: From the time spectrum of delayed coincidences in ^{35}Al β^- decay (2001Nu01).
1689 *3*	1/2$^+$		E	J$^\pi$: L(n)=0 in ^{9}Be(^{36}Si,^{35}Siγ).
1970 *6*			E	
2044 *5*	(1/2)$^-$		DE	J$^\pi$: L(d,p)=1 in ^{2}H(^{34}Si,pγ), 1/2$^-$ from shell-model predictions. Configuration=νp$_{1/2}$.
2168.2 *4*	5/2$^+$		A E	J$^\pi$: corresponding to an IAR in ^{35}P with L(p)=2 and J=5/2$^+$ from R-Matrix analysis in ^{1}H(^{34}Si,p):From IAR (2012Im01).
2275 *6*			E	
2377 *7*			E	
3140			A	
3450			A	
3611? *8*			E	XREF: E(3611?)
3770			A	
5190			A	
≈5500	(5/2)$^-$		D	J$^\pi$: L(d,p)=3 in ^{2}H(^{34}Si,pγ). Configuration=νf$_{5/2}$.
5760			A	
6330			A	
7360			A	
7690			A	

[†] From a least-squares fit to γ-ray energies if applicable. Values without uncertainties are from ^{35}Al β^- decay, unless otherwise noted.
[‡] From shell mode predictions and systematic trends on Si isotopes.

$\gamma(^{35}Si)$

E$_i$(level)	J$_i^\pi$	E$_\gamma$[†]	I$_\gamma$[†]	E$_f$	J$_f^\pi$	Mult.	Comments
909.95	(3/2)$^-$	910.11 *30*	100	0	(7/2)$^-$		E$_\gamma$: others: 910 *3* from (^{34}Si,pγ) and 908 *4* from (^{36}Si,^{35}Siγ).
973.88	(3/2$^+$)	64.1 *3*	100	909.95	(3/2)$^-$		B(E1)(W.u.)=0.00036 *4*
		973.78 *20*	11.8 *24*	0	(7/2)$^-$	[M2]	B(M2)(W.u.)=0.059 *14*
1689	1/2$^+$	715[‡] *4*	14.6[‡] *16*	973.88	(3/2$^+$)		
		780[‡] *4*	100[‡] *8*	909.95	(3/2)$^-$		
1970		1970[‡] *6*	100	0	(7/2)$^-$		
2044	(1/2)$^-$	1134[‡] *5*	100	909.95	(3/2)$^-$		E$_\gamma$: from (^{36}Si,^{35}Siγ). Other: 1134 *6* from (^{34}Si,pγ).
2168.2	5/2$^+$	1194.2 *4*	35 *8*	973.88	(3/2$^+$)		
		2168.2 *6*	100 *20*	0	(7/2)$^-$		E$_\gamma$: other: 2164 *6* from (^{36}Si,^{35}Siγ). I$_\gamma$: from ^{35}Al β^- decay (38.1 ms).
2275		2275[‡] *6*	100	0	(7/2)$^-$		
2377		2377[‡] *7*	100	0	(7/2)$^-$		
3611?		3611[‡] *8*	100	0	(7/2)$^-$		

[†] From ^{35}Al β^- decay, unless otherwise noted.
[‡] From ^{9}Be(^{36}Si,^{35}Siγ).

Adopted Levels, Gammas

Level Scheme

Intensities: Relative photon branching from each level

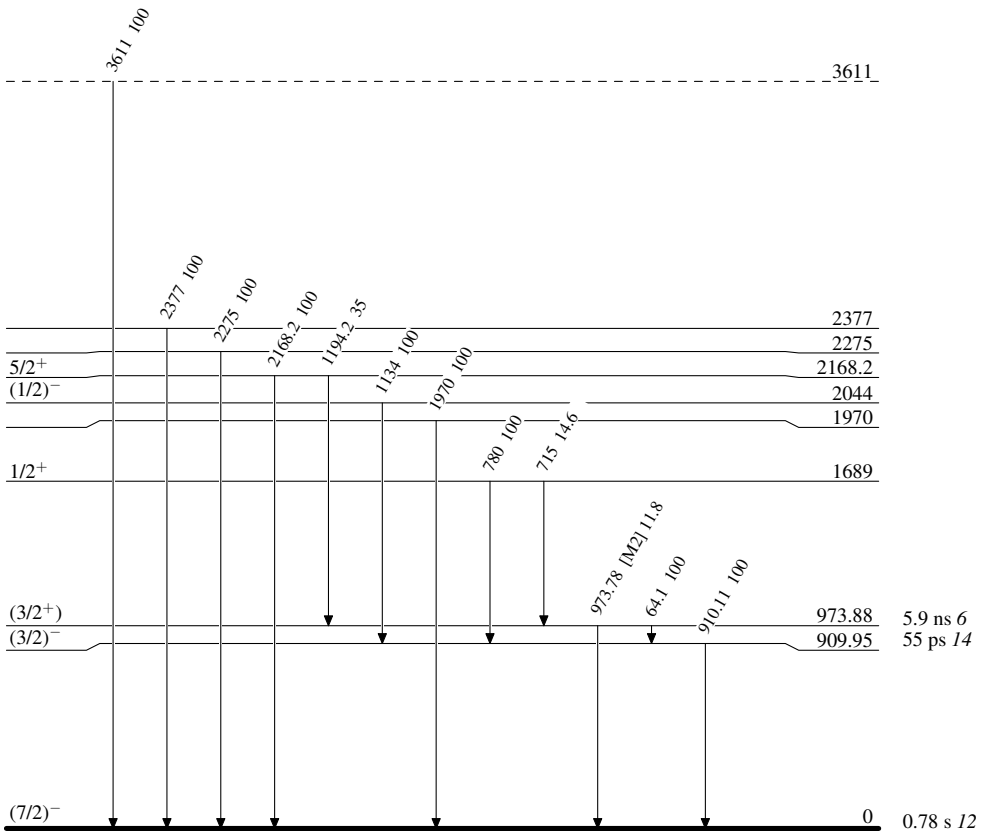

$^{35}_{14}Si_{21}$